



Original Research Article

KHDC3 affects the lineage differentiation of early embryo by regulating the differential distribution of YAP signal

Qian Xu^{a,1}, Yuling Lin^{b,1}, Lina Yu^a, Yang Zhang^a, Na Kong^a, Guijun Yan^{a,b,c,d},
Haixiang Sun^{a,*}, Guangyi Cao^{a,b,c,d,*}

^a Center for Reproductive Medicine and Obstetrics and Gynecology, Nanjing Drum Tower Hospital, Affiliated Hospital of Medical School, Nanjing University, Nanjing, 210008, China

^b State Key Laboratory of Reproductive Medicine and Offspring Health, Center for Reproductive Medicine and Obstetrics and Gynecology, Nanjing Drum Tower Hospital Clinical College of Nanjing Medical University, Nanjing, 210008, China

^c Center for Molecular Reproductive Medicine, Nanjing University, Nanjing, 210008, China

^d Jiangsu Human Reproductive Function Remodeling Engineering Research Center, Nanjing, 210008, China

ARTICLE INFO

Keywords:

Hydatidiform mole
Embryo
Cell lineage
Khdc3
YAP

ABSTRACT

Hydatidiform mole (HM) is characterized by abnormal fetal tissue loss and placental villous trophoblastic hyperplasia, indicating aberrant early embryonic cell fate differentiation. Clinical observations linking KH Domain Containing 3 (KHDC3) mutations to complete hydatidiform mole (CHM) suggest a potentially unforeseen role for KHDC3 in early embryonic development. Single-cell transcriptome analysis of early embryos revealed notable heterogeneity in KHDC3 expression levels from the 8-cell to blastocyst stage. Initial investigations indicated that varying KHDC3 expression levels at the 8-cell stage could influence the Yes-associated protein (YAP) signaling pathway. Knocking down KHDC3 in individual blastomeres at the 2-cell stage resulted in reduced blastocyst formation rates. *Khdc3*-knockdown (*Khdc3*-KD) embryos exhibited disruptions in embryonic cell lineage differentiation, characterized by decreased expression of the inner cell mass (ICM) marker organic cation/carnitine transporter 4 (OCT4) and diminished differential expression of the trophectoderm (TE) marker caudal type homeobox 2 (CDX2). The nuclear entry of phosphorylated YAP in outer cells is pivotal for inducing lineage differentiation. Intriguingly, in *Khdc3*-KD morulae, a significant reduction in the nuclear entry of phosphorylated YAP in outer cells was observed. Moreover, KHDC3 knockdown simultaneously impaired cortical actin cap formation during the morula stage. Forces generated at the apical cortex during this process segregate cells into inner and outer positions within the embryo, thereby influencing ICM versus TE fate specification. Our research underscores the role of KHDC3 in modulating the YAP signaling pathway to establish distinct inner and outer cell distributions during the morula stage, consequently influencing early embryonic lineage differentiation. Nevertheless, the precise mechanism by which KHDC3 influences the YAP signaling pathway via the actin cytoskeleton remains to be fully elucidated. Given the severity of recurrent miscarriages associated with KHDC3 mutations, elucidating the distinctive role of KHDC3 in early embryonic development warrants further investigation.

1. Introduction

Hydatidiform mole (HM), one of the most common gestational trophoblast diseases, is primarily characterized by abnormal fetal development or tissue loss, accompanied by placental villous

trophoblastic hyperplasia and pronounced interstitial edema [1,2]. Epidemiological studies indicate significant regional variation in HM incidence worldwide, ranging from 0.2 to 9.9 per thousand pregnancies [3]. In North America and Europe, the estimated incidence is 60–120 cases per 100,000 pregnancies [4]. However, higher rates are observed

* Corresponding author. 321 Zhongshan Road, Gulou District, Nanjing City, Jiangsu Province, 210008, China.

** Corresponding author. Center for Reproductive Medicine and Obstetrics and Gynecology, Nanjing Drum Tower Hospital, Affiliated Hospital of Medical School, Nanjing University, Nanjing, 210008, China.

E-mail addresses: haixiang_sun@nju.edu.cn (H. Sun), caogy@njglyy.com (G. Cao).

¹ These authors contributed equally to this work.

in Asia, potentially linked to genetic factors, with reported incidences of approximately 0.5 % in China, 1.3 % in Indonesia, and 0.19–0.49 % in Japan [5–9]. Consequently, HM poses a serious threat to female fertility.

Among HM subtypes, complete hydatidiform mole (CHM) is characterized by trophoblastic proliferation and complete deletion of the epiblast (EPI). These evidences suggest abnormal lineage differentiation during the development of human CHM. Following zygotic genome activation, differences emerge between embryonic cells, eventually forming three distinct cell lineages: the extraembryonic trophoblast (TE), the primitive endoderm (PrE), and the embryonic EPI. They are specified by undergoing two rounds of separation [10]. The first lineage separation was marked by the differentiation of blastomeres into the inner cell mass (ICM) and TE between morula and blastocyst. The embryo begins to show polarity during this stage. In the outer cells of the embryo, unphosphorylated Yes-associated protein 1 (YAP1) is translocated into the nucleus and interacts with TEA domain family member 4 (TEAD4) transcription factors to promote TE-specific gene expression, including caudal type homeobox 2 (*Cdx2*) and GATA binding protein 3 (*Gata3*) and inhibit the expression of pluripotency related genes sex determining region Y-box 2 (*Sox2*) [11–14]. In inner cells, phosphorylated YAP1 is confined outside the nucleus, preventing the induction of TE-specific gene expression [13]. Lineage tracing of mice showed that TE produced the placenta, and ICM produced all tissues of the fetus and some outer membrane tissues of the embryo [15]. During the second lineage separation, ICM would separate into PrE and EPI. PrE-cells mainly develop into the extraembryonic endoderm layers of the visceral and parietal yolk sacs after implantation in mice, while EPI cells are pluripotent and eventually constitute fetal tissue [10,16,17].

While the precise cause of abnormal lineage differentiation in CHM remains unclear, maternal gene mutations are identified as the most significant risk factor for familial recurrent hydatidiform mole. In 2011, Parry and his colleagues found that KH domain containing 3-like (*KHDC3*) gene mutation could lead to recurrent hydatidiform mole [18]. Approximately 10–14 % of biparental hereditarily CHM is related to *KHDC3* mutations. Besides, several different *KHDC3* mutation sites, leading to recurrent hydatidiform mole, has been reported so far [18–20]. However, the pathogenesis of human recurrent hydatidiform mole caused by *KHDC3* gene mutation remains poorly understood.

Current studies of *KHDC3* mainly focus on its role during oocyte maturation. For example, *KHDC3* has been identified as one of the main components of the human subcortical maternal complex (SCMC). The SCMC complex consists of several maternal protein [21]. SCMC is a key protein complex essential for oocyte maturation, oocyte zygotic transition and embryo development [21]. Furthermore, *KHDC3* can interact with poly(ADP-ribose) polymerase 1 (PARP1), stimulating its enzymatic activity and thereby reducing DNA damage in mouse embryonic stem cells [22–24].

This project focuses on investigating the critical role of *Khdc3* in the lineage differentiation and embryo polarity during early mouse embryonic development, according to the typical feature of trophoblast hyperplasia in human CHM. We aim to determine whether the loss of *Khdc3* affects blastomere cell fate decisions during embryo lineage differentiation. We hypothesize that, following the completion of maternal-to-zygotic transition at the 2-cell stage, the absence of *KHDC3* would disrupt embryonic lineage differentiation from the 8-cell stage to the blastocyst stage. This disruption may provide a mechanistic explanation for why *KHDC3* mutations cause CHM. Our goal is to elucidate the mechanism of HM caused by *KHDC3* mutation, providing insights for the clinical diagnosis and treatment of recurrent HM and informing genetic counseling.

2. Materials and methods

2.1. Experimental design

Following data analysis revealing the expression trend of *KHDC3*,

subsequent experiments were designed to specifically ablate its significant influence from the 2-cell to blastocyst stage. This design was motivated by both the observed differential expression of *KHDC3* between blastomeres and established reports highlighting its critical role in the oocyte-to-embryo transition (oocyte to zygote) [25]. Embryos of consistent quality were obtained via IVF. To experimentally induce asymmetry between blastomeres, control siRNAs or *Khdc3*-targeting siRNAs was microinjected into single blastomere at the late 2-cell stage. This timing was chosen to ensure complete separation of the two blastomeres. Embryos were injected with control siRNAs served as the control group, while those injected with *Khdc3*-targeting siRNA constituted the *Khdc3*-knockdown group. Following injection, embryos were cultured further and collected at the E3.5 and E4.5 stages for evaluation. These embryos were subjected to immunofluorescence, quantitative RT-PCR, and transcriptome sequencing analyses to comprehensively assess the impact of *KHDC3* knockdown on early embryonic development. Fig. 4A was the experimental design diagram.

2.2. Animals

All animal experiments were conducted in accordance with the guidelines of the Animal Care and Use Committee of Nanjing Drum Tower Hospital (2025AE01013). The C57BL/6 mice were purchased from Beijing Vital River Laboratory Animal Technology Company. The mice were fed a regular diet and placed in a room with a 12:12-h light-dark cycle control at 22 °C strictly.

2.3. Embryo acquisition and culture

The methods for embryo acquisition and culture refer to the article already published by the previous research [26]. 8-week-old female B6D2F1 mice and 12-week-old male B6D2F1 mice were used in the IVF experiments. Female mice were treated with 10 IU of serum gonadotropin (Ningbo Sansheng Biotechnology Co., LTD., Veterinary drug No. 110914564). After 48 h, these mice were injected with 10 IU chorionic gonadotropin (Ningbo Sansheng Biotechnology Co., LTD., Veterinary medicine word 110911282) for superovulation. Fifteen hours after chorionic gonadotropin injection, MII oocytes were collected from the ampulla of the fallopian tube and transferred to G-IVF™ PLUS supplemented with HSA (Vitrolife Sweden, REF 10136, Balance overnight at 37 °C and 5 % CO₂ before use). For 1h after the capacitation of sperm, the MII oocytes of female B6D2F1 mice were fertilized with epididymal sperm of male B6D2F1 mice in the G-IVF™ PLUS. Four to 6 h after fertilization, the fertilized oocytes were washed and cultured in the G-1™ PLUS supplemented with HAS (Vitrolife Sweden, REF 10128, overnight equilibrium at 37 °C, 5 % CO₂ before use). The embryos used in the experiment were all of high quality and had the same developmental starting point. The embryos of zygotic, two-cell, four-cell, eight-cell, morula and blastocyst stages were collected at 8h, 24h, 36h, 48h, 60h and 72h after fertilization, respectively.

2.4. Antibodies

The following antibodies were used in this study. ECAT1/*KHDC3* antibody (AP11238a; dilution: IF 1:200; WB 1:1000; Abcepta). Rhodamine-Phalloidin (YP0063-50T; dilution IF 1:300; US EVER-BRIGHT® INC). ProLong™ Gold AntiFade with DAPI (P36931; Invitrogen). OCT4 (ab181557; dilution 1:300; abcam). *CDX2* Antibody (3977; dilution 1:200; Cell signaling technology). YAP (AB535096; dilution 1:200; Abnova). Phospho-YAP(Ser127) (PA5-114675; dilution 1:200; Thermo Fisher Scientific). β -Actin Mouse Monoclonal Antibody (AF0003; dilution 1:2000; Beyotime). Anti-mouse IgG Antibody (ZB2305; dilution 1:10000; Nakasugi Golden Bridge). Alexa Fluor 488 goat anti-rabbit IgG (A11008; dilution 1:1000; Thermo Fisher Scientific). Alexa Fluor 594 donkey anti-mouse IgG (A21203; dilution 1:1000; Thermo Fisher Scientific).

2.5. Microinjection

Mouse embryos were microinjected with about 10 pl siRNA (25 μ M), a mix pool of three sequence, through FemtoJet microinjector (Eppendorf, Germany) during the 2-cell stage. The siRNA was purchased, diluted with RNase-free water and stored at -80°C .

The siRNA 5'-3' sequence of *Khdc3* is as follows: F1: GCAGCUAUGUCAUAGUUCATT, R1: UGAACUAUGACAUCAGCUGCTT; F2: CCCUGAUCACUAGUGAACGUTT, R2: ACGUUCACAUGUAUCAGGGTT; F3: CAAGGUACCUAAUUGAAATT, R3: UUUCAAAUAAGGUACCUUGTT. The control embryos were injected with control siRNAs (GenePharma, China). The embryos were cultured in an incubator at 37°C (5 % O_2 , 5 % CO_2 , 90 % N_2) and keep recorded.

2.6. Immunofluorescence

Embryo were fixed at room temperature with PBS containing 4 % paraformaldehyde (PFA) for 30 min. The samples were then permeated with 0.5 % Triton X-100 at room temperature for 20 min and blocked with PBS containing 5 % FBS at room temperature for 1 h. The primary antibody was incubated at 4°C overnight, and washed with PBST (PBS containing tween-20) three times. The secondary antibody was incubated at room temperature and shielded from light for 1 h. The embryos were washed three times without light. The embryo sample was placed on a slide and sealed with ProLongTM Gold anti-quenching tablet (including DAPI). Imaging was performed using a laser scanning confocal microscope (Leica STELLARIS, Germany). Photos were taken using z stacks. Continuous images were obtained from the presence of a positive signal until the positive signal disappears and then superimposed. The software that comes with Leica was used to measure the fluorescence intensity.

2.7. Quantitative RT-PCR

Single cell sequence specific amplification kit (P621; Vazyme) was used to achieve embryo cDNA according to the instructions. The primers to be tested were mixed into a primer pool (the final concentration of each is 0.1 μ M). Ten morulas were used in average in each sample group. Embryos that degenerated due to the injection operation itself were all excluded. The reaction system of cell sample and primer pool was configured in the Nuclease-free centrifuge tube, and amplification was performed according to the 16 cycles as suggested. The cDNA was used for subsequent differential gene expression analysis. The cDNA was used for fluorescence quantitative PCR on LightCycler 480 II (Roche). Gene expression was normalized to 18s. The expression level of the gene was determined by $2^{-\Delta\Delta\text{Ct}}$. The primers used in qPCR were listed in Table S1.

2.8. RNA-seq

The RNA-seq library was established using commercial kits (N712; Vazyme; TD503; Vazyme). The embryos after microinjection at the 2-cell stage were cultured till morula stage. Each sample contained five morulae. Three samples were collected in both control and *Khdc3*-KD group and cleaved with 18 μ L lysis buffer containing 2 μ L RNase inhibitor (all provided by N712 kit). Full-length cDNA was amplified using N712 kit. According to the recommendations in the instruction manual, 15 cycles were used for full-length cDNA amplification. After that, 1 ng DNA was recommended as the guidance to prepare DNA library using TD503 kit. The library was sequenced using Illumina HiSeq X Ten platform. The differentially expressed genes were analyzed and normalized using R package Deseq-2 (v1.28.1). Gene enrichment analysis of different-expressed transcripts was performed on David platforms (<https://david.ncifcrf.gov/>) and Metascape (<https://metascape.org/>) [27–29].

2.9. Immunoprecipitation-mass spectrometry (IP-MS)

Ovaries were collected from 3-week-old ICR female mice 44–46 h after injection of PMSG. Every group contained 10 ovaries. The steps of IP are briefly described as follows: Beads were used to pre-clean the lysis first. The KHDC3 antibody and IgG were each incubated with ovarian lysate, and then magnetic beads are added to obtain complexes. The coprecipitated proteins were then analyzed by mass spectrometry (Thermo ScientificTM QExactiveTM HFX). The mass spectrometry data were studied using Proteome Discovery 2.4.

2.10. Statistical analysis

Student's t-test was used to evaluate differences between 2 groups. Multiple comparisons between more than 2 groups were analyzed by one-way ANOVA followed by Tukey's honest significant difference (HSD) test using Prism 5.0. The differences of $P \leq 0.05$ were considered to be significant. Data are expressed as mean \pm SEM from at least three independent experiments.

3. Results

3.1. Expression of KHDC3 in early human embryonic development

Considering that *KHDC3* mutations can lead to recurrent hydatidiform mole, we first reviewed the reported phenotypic consequences of these mutations. In addition to recurrent HM and recurrent pregnancy loss, *KHDC3* mutations also result in early embryonic developmental arrest (Fig. 1A,B) [30]. Combining the main clinical manifestations of recurrent hydatidiform mole, characterized by excessive proliferation of trophoblast layer and absence of epiblast, these phenotypes collectively suggest that *KHDC3* may disrupt lineage differentiation during early embryonic development.

To comprehensively characterize the dynamic expression pattern of *Khdc3* during early embryonic development, we reanalyzed the ribosome profiling sequencing data of *Khdc3* and SCMC major components at various stages of early embryonic development (GSE165782) [31]. We found that the expression of other major SCMC components peaked before the 4-cell stage. In contrast, *Khdc3* exhibited minimal expression before the 4-cell stage, initiated expression from the 8-cell stage, and increased significantly in ICM (Fig. 2A). Integration of single-cell transcriptomic data from individual blastomeres (GSE45719) [32] confirmed that *KHDC3* indeed began to express from the 8-cell stage at the single blastomere level, persisting until the late-blastocyst stage (Fig. 2B–D).

3.2. The differential expression of KHDC3 between different blastomeres affects the activation of the YAP/TAZ signaling pathway

From the 8-cell stage, *Khdc3* expression became increasingly heterogeneous between blastomeres, and this differential expression continued to expand until the late-blastocyst stage (Fig. 3A). To quantify single-cell variability, we compared standard deviations of *Khdc3* expression within individual embryos across developmental stages. Importantly, despite the increase in *Khdc3* expression at the single-cell level, the standard deviation of *Khdc3* within individual embryos also significantly increased (Fig. 3B and C).

To further elucidate the reason for the differentiation of *Khdc3* within the 8-cell stage, we compared the transcriptomic differences between *Khdc3*-high and *Khdc3*-low blastomeres at the 8-cell stage. We found that genes stimulated by YAP/TAZ signaling pathway were significantly activated in *Khdc3*-high cells (Fig. 3D and E).

Moreover, *Khdc3* exhibited varying expression levels in different cells of each blastocyst (Fig. S1A). Through gene ontology enrichment analysis in different cells, it was observed that differentially expressed genes were primarily involved in cellular response to DNA damage

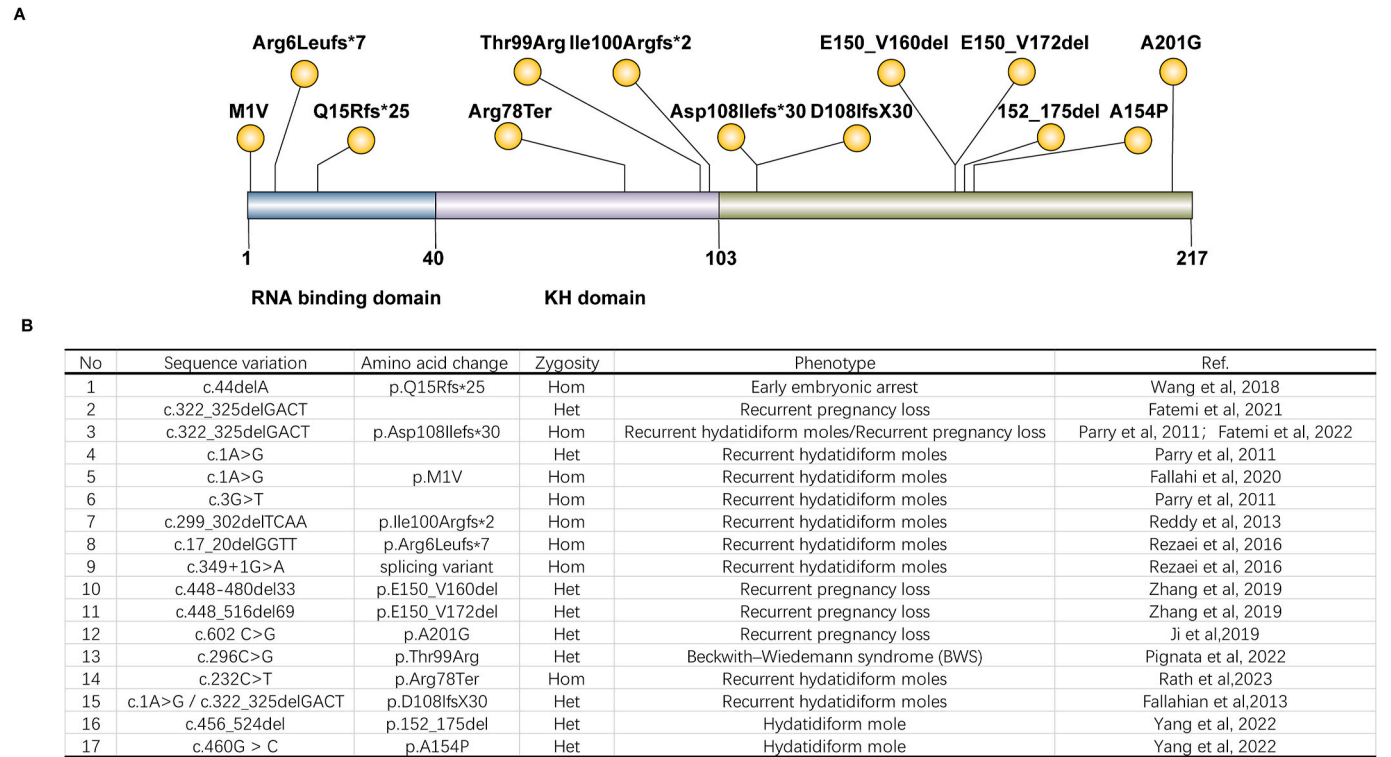


Fig. 1. | Summary of abnormal early human embryonic development caused by clinical KHDC3 mutations (A) Identified sites of KHDC3 mutations reported in clinical cases. (B) Tabulated data on mutation sites, amino acid alterations, zygosity, associated phenotypes, and relevant studies.

stimulus (Fig. S1B and S1C).

3.3. Knockdown of *Khdc3* in a single blastomere of two-cell embryos disrupts early embryonic development

To further elucidate the impact of differential *Khdc3* expression in individual blastomeres on early embryonic development, we micro-injected *Khdc3*-targeted siRNA into single blastomeres of 2-cell mouse embryos (Fig. 4A). This manipulation led to a significant decrease in *Khdc3* mRNA expression in the *Khdc3*-knockdown (*Khdc3*-KD) morulae, with immunofluorescence confirming diminished KHDC3 protein at the eight-cell stage (Fig. 4B–D). In examining the distribution of KHDC3 in eight-cell embryos, we assessed the fluorescence intensity of KHDC3 along an axis passing through the central point of the embryo. The X-axis denoted the distance to the subcortical region of the morula, while the Y-axis represented the fluorescence intensity of KHDC3. Compared to the control group, the *Khdc3*-KD group exhibited significantly reduced fluorescence intensity both at the central region and near the periphery of the embryo (Fig. 4E–G). *Khdc3*-KD embryos exhibited relative developmental delays. In comparison to the control group, the *Khdc3*-KD morulae exhibited a lower rate of blastocyst formation at 84 h post-fertilization. Furthermore, at 96 h post-fertilization, the *Khdc3*-KD embryos showed a higher rate of embryonic degeneration (Fig. 4H–I).

3.4. Transcriptome sequencing revealed abnormalities in cell polarity and lineage differentiation pathways in *Khdc3*-KD morulae

Transcriptome suggests that, in comparison to the control group morulae, the *Khdc3*-KD morulae exhibited significant upregulation of 360 genes and downregulation of 713 genes (Fig. 5A–C). Gene set enrichment analysis (GSEA) revealed upregulation of pathways including “mitotic cell cycle arrest”, “establishment of epithelial cell polarity” and “regulation of trophoblast cell migration”, while “cell fate specification” was significantly suppressed (Fig. 5D–G). These pathways are closely related to early embryonic lineage differentiation. Further

validation through q-RT-PCR confirmed the altered expression of genes associated with embryonic differentiation and development. It was observed that the expression of genes related to “cell fate specification,” such as *Oct4* and *Wnt3a*, was reduced in the *Khdc3*-KD group (Fig. 5H). To further elucidate how *Khdc3* regulates early embryonic lineage differentiation, considering the challenges in obtaining embryos and the abundant expression of *Khdc3* in oocytes, immunoprecipitation and mass spectrometry were employed to identify potential proteins interacting with KHDC3 in the ovary. Among these proteins, those linked to pluripotency may warrant special attention, as these pluripotency genes are also involved in epiblast formation and lineage differentiation (Fig. 5I).

3.5. *Khdc3* knockdown inhibits the formation of ICM in E3.5 blastocyst

To elucidate the impact of *Khdc3* knockdown on the formation of the ICM, we investigated the expression of OCT4, a crucial transcription factor for the ICM (Fig. 6A). The overall expression of OCT4 was significantly decreased in E3.5 embryos in the *Khdc3*-KD group. Furthermore, both the quantity and the percentage of OCT4-positive cells in E3.5 embryos exhibited a significant reduction in the *Khdc3*-KD group (Fig. 6B–D).

3.6. *Khdc3* knockdown affected the differentiation of trophoblast cells in E4.5 blastocyst

Following *Khdc3* knockdown, only a small portion of blastocysts could hatch. This raises the question of whether these hatching blastocysts exhibit abnormalities in lineage differentiation. To investigate the impact of *Khdc3* knockdown on trophoblast cell differentiation, we focused on CDX2, a transcription factor specific to trophoblast cells, in E4.5 blastocysts and measured the fluorescence intensity of CDX2 per cell in each embryo (Fig. 7A). While the expression of CDX2 was slightly reduced in *Khdc3*-KD blastocysts, the standard deviation of CDX2 expression in each cell showed significant variation (Fig. 7B,C).

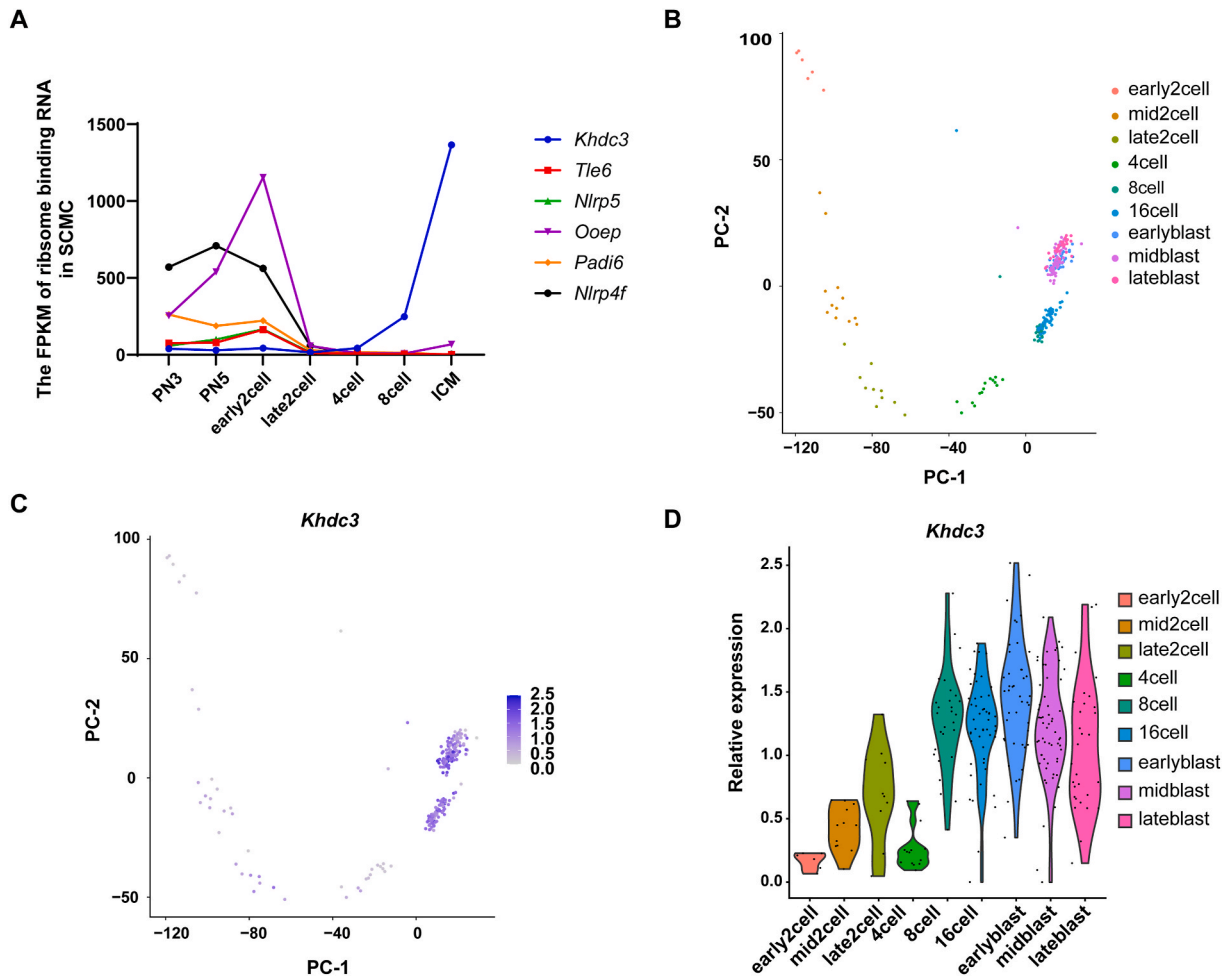


Fig. 2. | KHDC3 Expression in pre-implantation early embryos (A) Expression levels of SCMC components in early mouse embryos inferred from ribosomal transcriptomes. PN3: pro-nucleus stage 3; PN5: pro-nucleus stage 5. (B) Principal Component Analysis (PCA) of mouse single-cell blastomeres at various early embryo developmental stages. (C) *Khdc3* expression in mouse single-cell blastomeres at different early embryo developmental stages. (D) Violin plot depicting the relative expression levels of *Khdc3* in individual blastomeres at different developmental stages of early mouse embryos.

3.7. *Khdc3* knockdown suppressed the differential expression and localization of YAP/p-YAP in inner and outer cells of the morula

Through immunofluorescence analysis, we confirmed the expression and phosphorylation status of YAP in both control and *Khdc3*-KD morulae (Fig. 8A). Evidently, in the control group, YAP was predominantly localized in the nucleus of outer cells, while phosphorylated YAP was confined outside the nucleus in the inner cells. However, in the *Khdc3*-KD morulae, this distinct distribution pattern was notably disrupted (Fig. 8A,B). Notably, the overall fluorescence intensity of YAP was diminished in the *Khdc3*-KD morulae (Fig. 8C). Moreover, the average fluorescence intensity of each cell in the *Khdc3*-KD morulae was significantly lower compared to the control group (Fig. 8D).

3.8. *Khdc3* knockdown altered the expression and distribution of F-actin in the morula

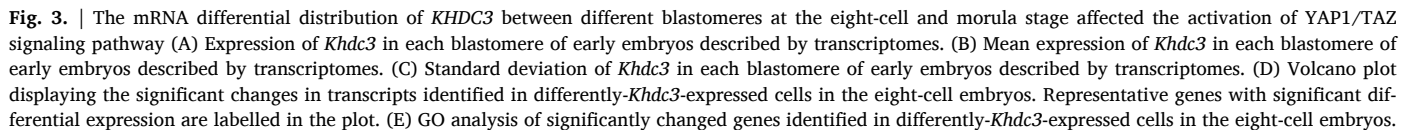
RNA-seq analysis of *Khdc3*-KD morulae revealed a significant down-regulation of the “positive regulation of actin filament bundle assembly” pathway (Fig. 9A). Immunofluorescence analysis confirmed a distinct reduction in the expression of F-actin, particularly in the *Khdc3*-KD group where abnormal cortical actin cap formation was evident, characterized by a decreased intensity of the actin cap (Fig. 9B–F).

4. Discussion

KHDC3 mutations represent a significant etiological factor in recurrent miscarriage and early embryonic arrest. However, the mechanistic basis for *KHDC3*-related developmental abnormalities remains unclear. This study focuses on investigating how *KHDC3* regulates early embryonic development through lineage specification and YAP/TAZ signaling modulation.

Through transcriptome analysis of individual blastomeres, we observed an increase in *Khdc3* expression post 8-cell stage, accompanied by expression variations among blastomeres. It is known that the 8-cell/morula stage is a critical period for blastomere polarity and cell fate determination [11–14]. Thus, our results may suggest a potential association between high *Khdc3* expression levels and cellular lineage differentiation. To further dynamically capture subtle changes of *KHDC3* at the single blastomere level, we carefully reanalyzed the data published. Our finding clearly indicates that *Khdc3* undergoes expression differentiation after the 8-cell stage. Genes stimulated by YAP/TAZ signaling pathway were significantly activated in *Khdc3*-high cells. The activation of the YAP/TAZ signaling pathway is crucial for embryonic polarization, indicating a potential association between the differential expression of *Khdc3* and cell polarization during the 8-cell stage.

Next, we herein proved that embryo with reduced *Khdc3* expression exhibited a significantly decreased rate of blastocyst formation. Clinically, recurrent miscarriages caused by *Khdc3* mutations are



According to our results, we considered that KHDC3 impacts the expression of lineage differentiation-related molecules by influencing the YAP/TAZ pathway. The differentiation of early embryonic lineages is highly regulated by the YAP/TAZ signaling pathway. YAP phosphorylation governs its movement between the nucleus and cytoplasm.

In addition, KHDC3 is an important component of SCMC. No

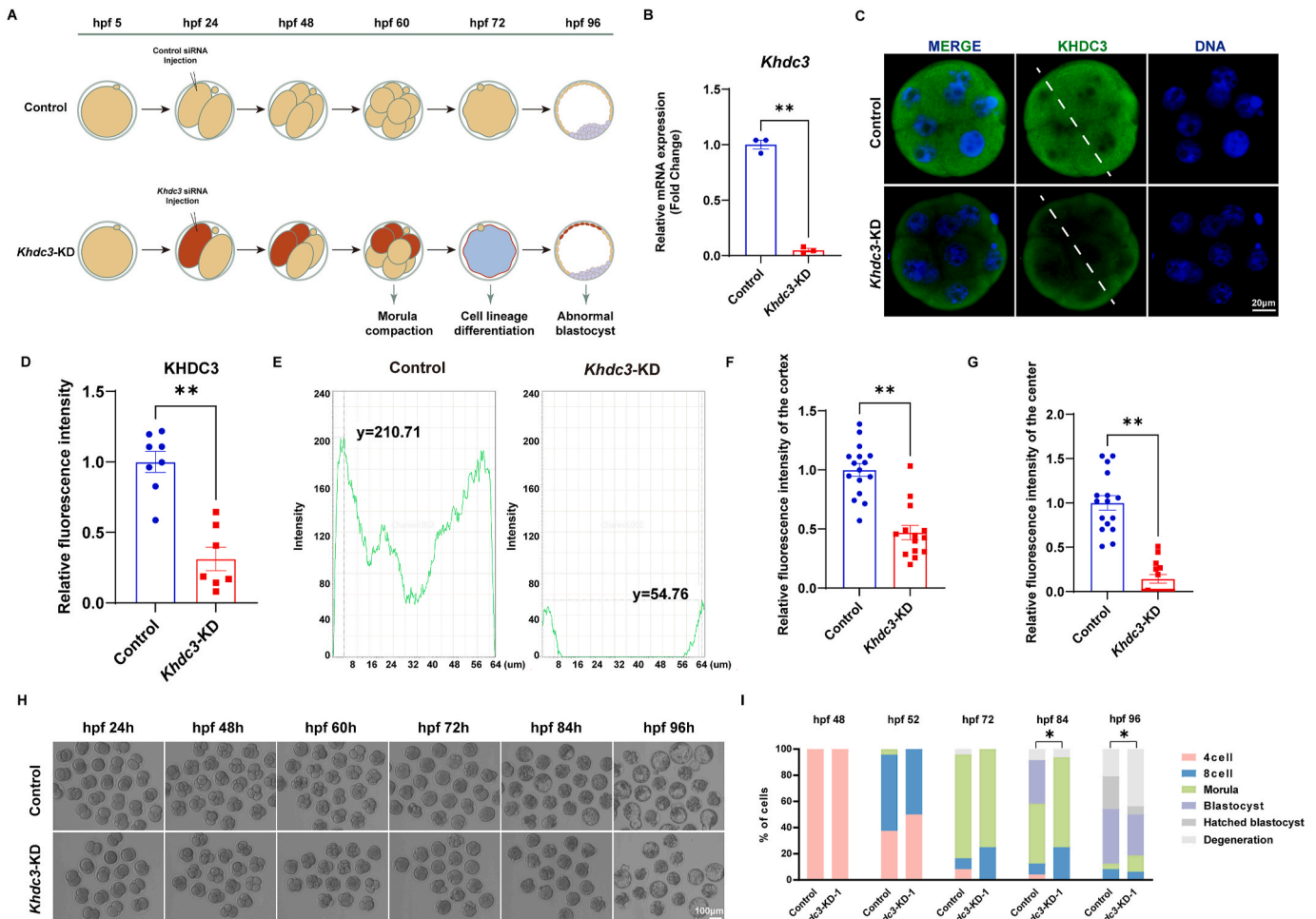


Fig. 4. | *Khdc3* knockdown affected the early embryonic development process (A) Experimental design diagram for *Khdc3* knockdown. Briefly, a mix of siRNA were injected into one cell of two-cell mouse embryo to achieve *Khdc3* single-cell knockdown embryo. hpf: hours post fertilization. (B) Expression of *Khdc3* mRNA in eight-cell embryos of two group (n = 3). **, $p < 0.01$. (C) Immunofluorescence staining showing the protein expression change in control group (n = 8) and *Khdc3*-KD group (n = 7). KHDC3, labelled in green. DNA, labelled in blue. (D) The relative fluorescence intensity of *Khdc3* expression in control group (n = 8) and *Khdc3*-KD group (n = 7) of eight-cell. **, $p < 0.01$. (E) The greyscale values of KHDC3 in eight-cell embryos are shown in the longitudinal section for both the control and *Khdc3*-KD groups, as depicted in the diagram. (F) The relative fluorescence intensity of KHDC3 of the embryo cortex in control group (n = 16) and *Khdc3*-KD group (n = 14) of eight-cell. **, $p < 0.01$. (G) The relative fluorescence intensity of KHDC3 of the embryo center in control group (n = 16) and *Khdc3*-KD group (n = 14) of eight-cell. **, $p < 0.01$. (H) Representative images of *Khdc3*-KD and control embryos at different developmental stages. Scale bar, 100 μm. (I) Bar graph representing the proportions of *Khdc3*-KD (n = 56) and control (n = 75) embryos at different developmental stages. hpf, hours post-fertilization. *, $p < 0.05$. (For interpretation of the references to colour in this figure legend, the reader is referred to the Web version of this article.)

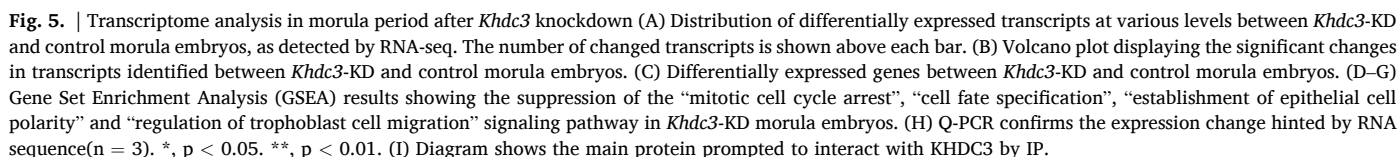
additional role of SCMC members in the early embryonic lineage differentiation was observed in our outcomes. As a maternal protein, the transcript is thought to be degraded during meiosis maturation but the protein persists during early embryonic development [43]. The fertility of female mice with *Khdc3* biallelic knockout was seriously decreased, which did not affect oocyte development, ovulation, fertilization, and two-cell ratio, but led to delayed embryo development and affected the number of morula and blastocyst [44]. *Khdc3* therein was considered important in maintaining embryo euploidy by involving in spindle formation and the spindle assembly checkpoint (SAC). Whether SCMC plays an important role in the determination of embryonic cell fate remains to be further studied.

Furthermore, it was observed in our study that at the blastocyst stage, cells with varying levels of *Khdc3* expression exhibited significantly different levels of pathways associated with DNA damage response. This may suggest that the differential expression of *Khdc3* in each cell of blastocyst may be linked to the DNA damage stimulus received and the varied response to DNA damage. The functional investigation of KHDC3 focuses on regulating DNA damage response

across multiple tiers. In studies involving embryonic stem cells (ESCs), KHDC3 was found to engage in cell cycle surveillance and DNA damage repair by interacting with PARP1, markedly enhancing PARP1 enzyme activity [22–24]. Additionally, KHDC3 plays a role in repairing damage at DNA double-strand break sites through a PARP1-independent pathway [45]. The involvement of KHDC3 in repairing DNA damage in Epiblast cells and maintaining genomic integrity necessitates further scrutiny.

5. Conclusion

In summary, we have established the significant heterogeneity in *Khdc3* expression levels among individual blastomeres from the 8-cell to blastocyst stages. KHDC3 influences the differentiation of early embryos by affecting the differential distribution of the inner and outer layers during the morula stage through the YAP pathway. Nonetheless, it remains uncertain whether KHDC3 impacts the YAP pathway by modulating the actin cytoskeleton. Given the severity of recurrent miscarriages resulting from KHDC3 mutations, the distinctive role of



original contributions presented in the study are included in the article/supplementary materials, and further inquiries can be directed to the corresponding author.

Institutional review board statement

The animal study was reviewed and approved by the Institutional Animal Care and Use Committee of Nanjing Drum Tower Hospital (2025AE01013).

Funding

This work was supported by National Natural Science Foundation of China (82471691), the State Key Laboratory of Reproductive Medicine and Offspring Health, Nanjing Medical University(SKLRM-2022D2), Clinical Trials from Nanjing Drum Tower Hospital, Affiliated Hospital of

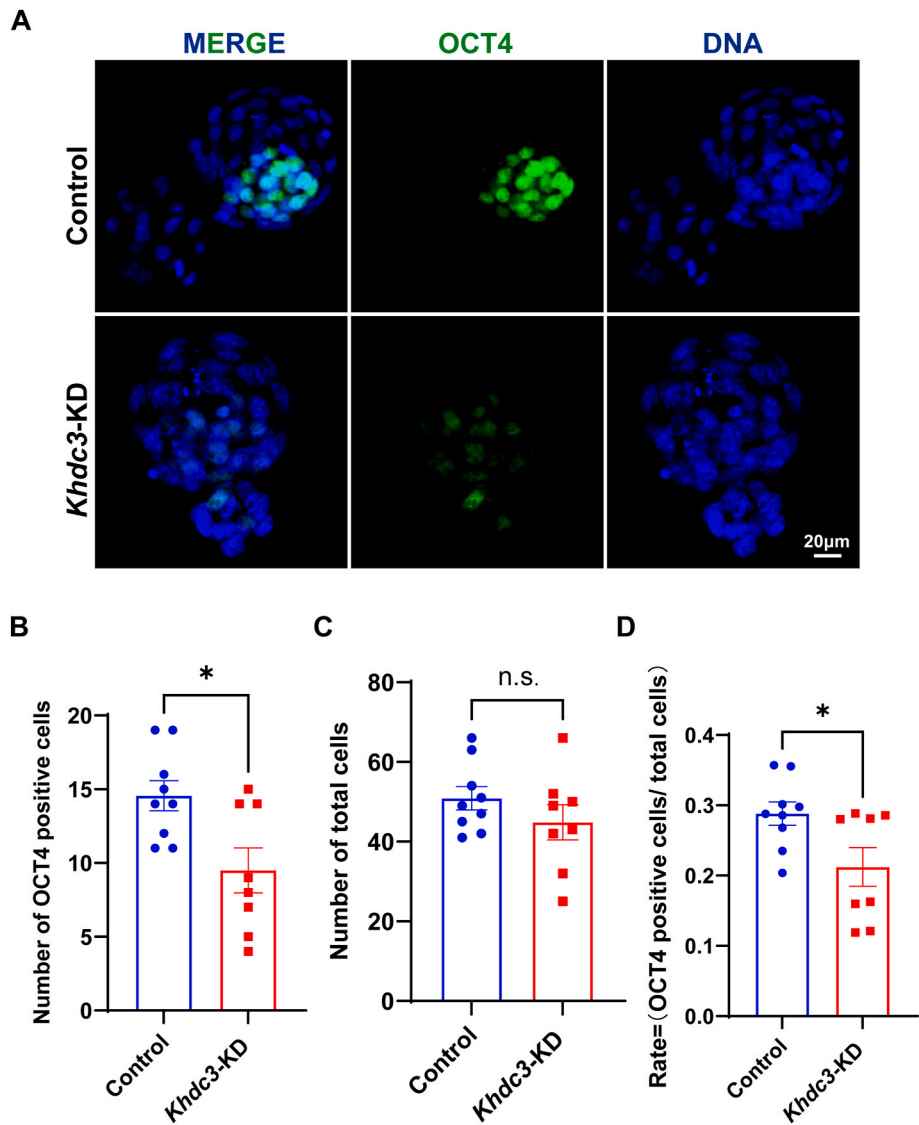


Fig. 6. | *Khdc3*-KD disrupted the inner cell mass differentiation of E3.5 embryo (A) Immunofluorescence staining showing the protein expression change in control group(n = 9) and *Khdc3*-KD group(n = 8). OCT4, labelled in green. (B) The number of OCT4 positive cells is counted. *, $p < 0.05$. (C) The number of total cells is counted. n.s., no significance. (D) The proportion of OCT4 positive cells to total cells is counted. *, $p < 0.05$. (For interpretation of the references to colour in this figure legend, the reader is referred to the Web version of this article.)

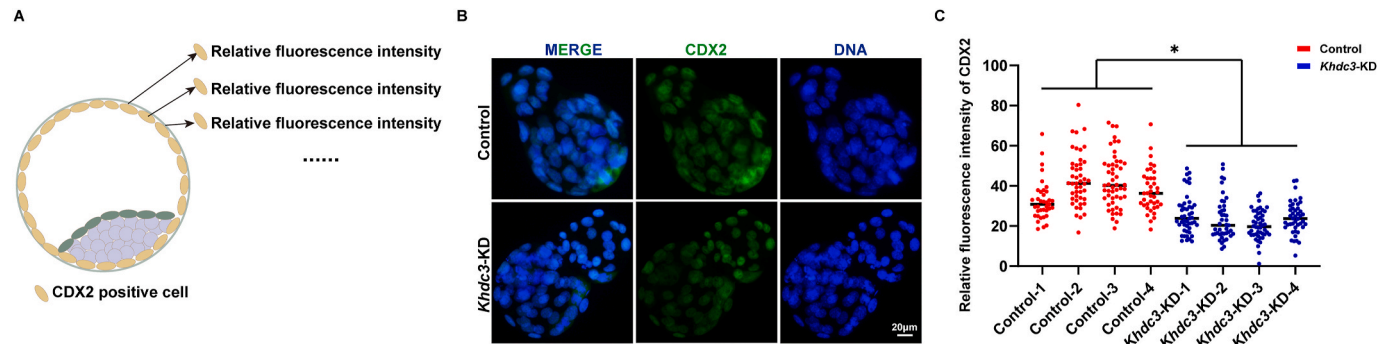


Fig. 7. | *Khdc3*-KD disrupted the trophoblast lineage differentiation of E4.5 blastocyst (A) Experimental design diagram for measurement of relative fluorescence intensity of CDX2. (B) Immunofluorescence staining showing the protein expression change in two groups. CDX2, labelled in green. DNA, labelled in blue. (C) Every point represents the relative intensity of CDX2 in a single cell of the embryo in control group(n = 3) and *Khdc3*-KD group(n = 4). The standard deviation of relative fluorescence intensity of CDX2 is calculated. *, $p < 0.05$. (For interpretation of the references to colour in this figure legend, the reader is referred to the Web version of this article.)

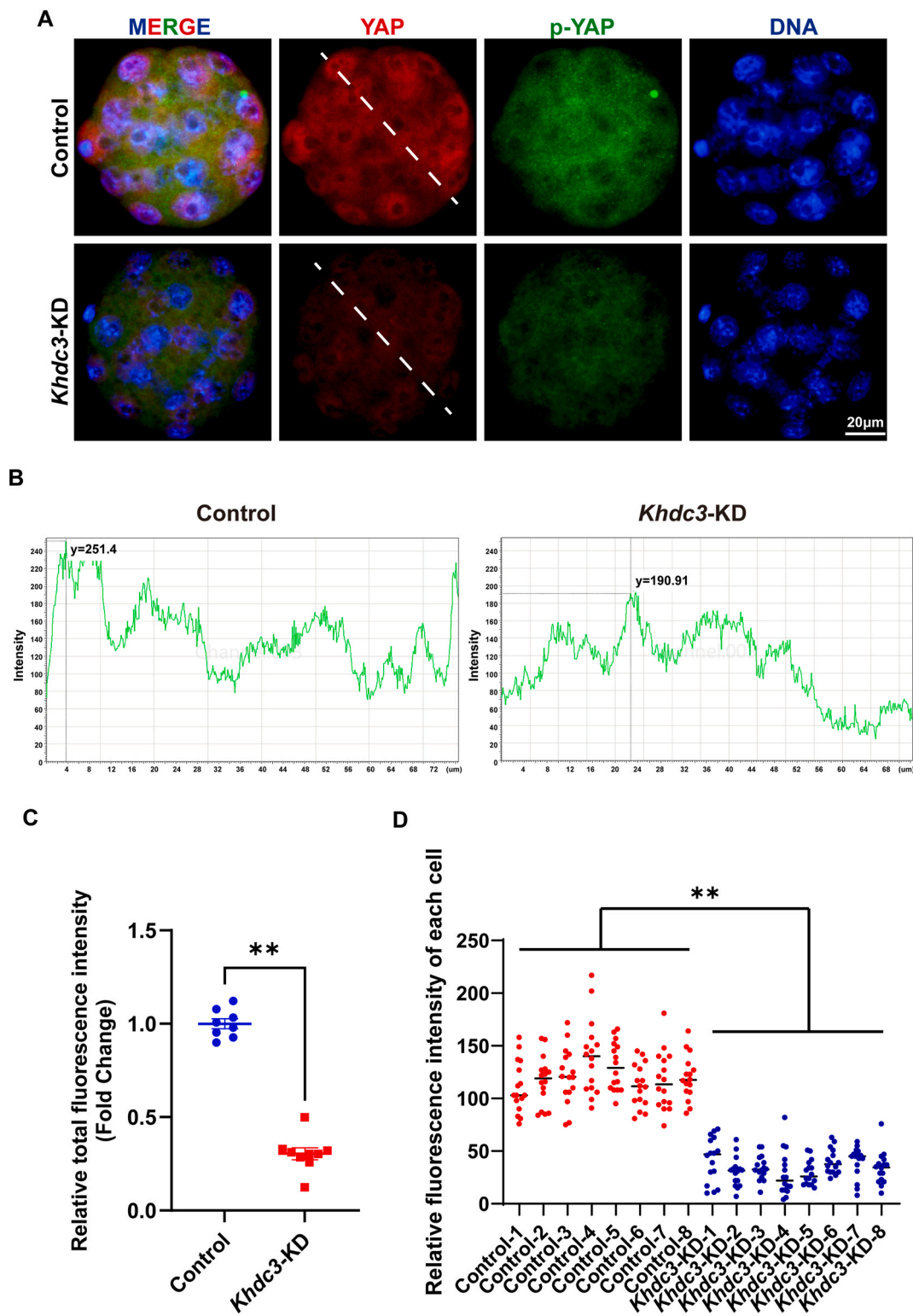


Fig. 8. | *Khdc3*-knockdown inhibited the differential expression and distribution of YAP/p-YAP between inner and outer cells (A) Immunofluorescence staining showing the protein expression change in control group(n = 8) and *Khdc3*-KD group(n = 8). p-YAP, labelled in green. YAP, labelled in red. (B) The greyscale values of YAP are shown in the longitudinal section for both the control and *Khdc3*-KD groups, as depicted in the diagram. (C) The relative fluorescence intensity of YAP expression in control group(n = 8) and *Khdc3*-KD group(n = 8). **, $p < 0.01$. (D) Every point represents the relative intensity of YAP in a single cell of the embryo. The average of relative fluorescence intensity of YAP is calculated. *, $p < 0.05$. (For interpretation of the references to colour in this figure legend, the reader is referred to the Web version of this article.)

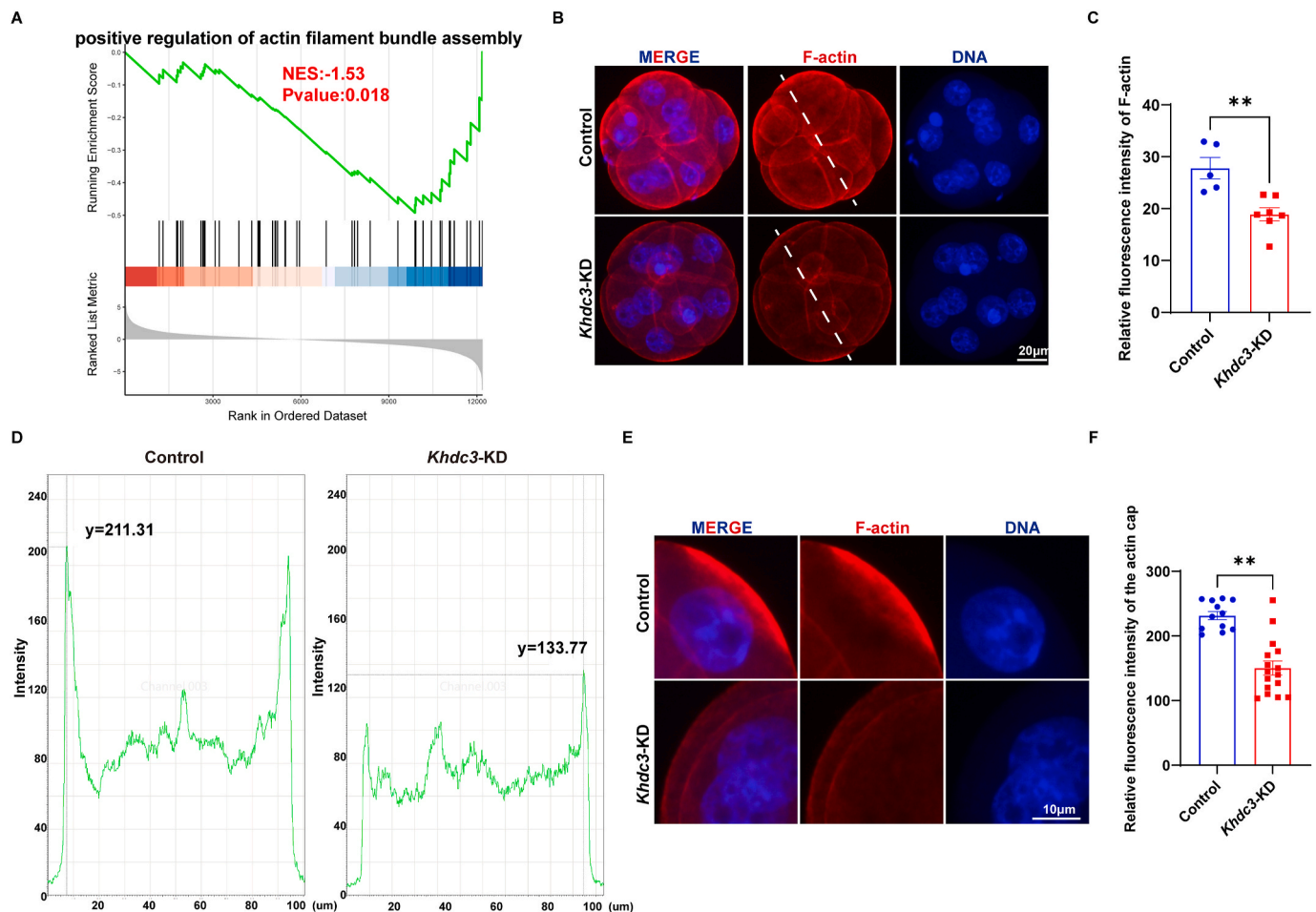


Fig. 9. | *Khdc3*-knockdown affected the expression and distribution of F-actin (A) Gene Set Enrichment Analysis (GSEA) results showing the suppression of the “positive regulation of actin filament assembly” signaling pathway in *Khdc3*-KD morula embryos. (B) Immunofluorescence staining showing the protein expression change in control group (n = 5) and *Khdc3*-KD group (n = 7). F-actin, labelled in red. DNA, labelled in blue. (C) The relative fluorescence intensity of F-actin expression in control group (n = 5) and *Khdc3*-KD group (n = 7). **, p < 0.01. (D) The greyscale values of F-actin are shown in the longitudinal section for both the control and *Khdc3*-KD groups, as depicted in the diagram. (E) Immunofluorescence staining showing part of the protein expression change in control group (n = 12) and *Khdc3*-KD group (n = 16). The actin cap is focused. F-actin, labelled in red. (F) The relative fluorescence intensity of actin cap of the embryo cortex in control group (n = 12) and *Khdc3*-KD group (n = 16). **, p < 0.01. (For interpretation of the references to colour in this figure legend, the reader is referred to the Web version of this article.)

Medical School, Nanjing University (2022-LCYJ-ZD-02, 2023-LCYJ-PY-35), Research Project of Changzhou Medical Center of Nanjing Medical University, Key Program (CMCM202203), and Key Medical Research Project of Jiangsu Province Health Commission (K2023058).

Declaration of competing interest

The authors declare that they have no known competing financial interests or personal relationships that could have appeared to influence the work reported in this paper.

Appendix A. Supplementary data

Supplementary data to this article can be found online at <https://doi.org/10.1016/j.theriogenology.2025.117527>.

References

- Hui P, et al. Hydatidiform moles: genetic basis and precision diagnosis. *Annu Rev Pathol* 2017;12:449–85.
- Moein-Vaziri N, et al. Clinical and genetic-epigenetic aspects of recurrent hydatidiform mole: a review of literature. *Taiwan J Obstet Gynecol* 2018;57(1): 1–6.
- Tantengco OAG, et al. Molar pregnancy in the last 50 years: a bibliometric analysis of global research output. *Placenta* 2021;112:54–61.
- Fiorea A, et al. Hydatidiform mole-between chromosomal abnormality, uniparental disomy and monogenic variants: a narrative review. *Life (Basel)* 2023;13(12).
- Shang ER. [A retrospective investigation on the incidence of hydatidiform mole in 20,548 fertile women]. *Zhonghua Yixue Zazhi* 1982;62(5):282–5.
- Song HZ, Wu PC. Hydatidiform mole in China: a preliminary survey of incidence on more than three million women. *Bull World Health Organ* 1987;65(4):507–11.
- Nakano R, et al. Trophoblastic disease: analysis of 342 patients. *Gynecol Obstet Invest* 1980;11(4):237–42.
- Takeuchi S. Incidence of gestational trophoblastic disease by regional registration in Japan. *Hum Reprod* 1987;2(8):729–34.
- Gonzalez J, et al. Gestational trophoblastic disease: complete versus partial hydatidiform moles. *Diseases* 2024;12(7).
- Qin J, et al. Mga safeguards embryonic stem cells from acquiring extraembryonic endoderm fates. *Sci Adv* 2021;7(4).
- Saini D, Yamanaka Y. Cell polarity-dependent regulation of cell allocation and the first lineage specification in the preimplantation mouse embryo. *Curr Top Dev Biol* 2018;128:11–35.
- Ralston A, et al. Gata3 regulates trophoblast development downstream of Tead4 and in parallel to Cdx2. *Development* 2010;137(3):395–403.
- Nishioka N, et al. The Hippo signaling pathway components Lats and Yap pattern Tead4 activity to distinguish mouse trophectoderm from inner cell mass. *Dev Cell* 2009;16(3):398–410.
- Frum T, Murphy TM, Ralston A. HIPPO signaling resolves embryonic cell fate conflicts during establishment of pluripotency in vivo. *eLife* 2018;7.
- Rossant J. Cell lineage analysis in mammalian embryogenesis. *Curr Top Dev Biol* 1987;23:115–46.

- [16] Gardner RL, Rossant J. Investigation of the fate of 4-5 day post-coitum mouse inner cell mass cells by blastocyst injection. *J Embryol Exp Morphol* 1979;52:141–52.
- [17] Kwon GS, Viotti M, Hadjantonakis AK. The endoderm of the mouse embryo arises by dynamic widespread intercalation of embryonic and extraembryonic lineages. *Dev Cell* 2008;15(4):509–20.
- [18] Parry DA, et al. Mutations causing familial biparental hydatidiform mole implicate c6orf221 as a possible regulator of genomic imprinting in the human oocyte. *Am J Hum Genet* 2011;89(3):451–8.
- [19] Reddy R, et al. Report of four new patients with protein-truncating mutations in C6orf221/KHDC3L and colocalization with NLRP7. *Eur J Hum Genet* 2013;21(9):957–64.
- [20] Nguyen NMP, et al. The genetics of recurrent hydatidiform moles: new insights and lessons from a comprehensive analysis of 113 patients. *Mod Pathol* 2018;31(7):1116–30.
- [21] Monk D, Sanchez-Delgado M, Fisher R. NLRPs, the subcortical maternal complex and genomic imprinting. *Reproduction* 2017;154(6):R161–70.
- [22] Zhao B, et al. Filia is an ESC-specific regulator of DNA damage response and safeguards genomic stability. *Cell Stem Cell* 2015;16(6):684–98.
- [23] Zhao B, et al. Mouse embryonic stem cells have increased capacity for replication fork restart driven by the specific Filia-Floped protein complex. *Cell Res* 2018;28(1):69–89.
- [24] Zhang W, et al. KHDC3L mutation causes recurrent pregnancy loss by inducing genomic instability of human early embryonic cells. *PLoS Biol* 2019;17(10):e3000468.
- [25] Xu C, et al. The subcortical maternal complex safeguards mouse oocyte-to-embryo transition by preventing nuclear entry of SPIN1. *Nat Struct Mol Biol* 2025. <https://doi.org/10.1038/s41594-025-01538-0>. Apr 17. Online ahead of print.
- [26] Lin Y, et al. GATAD2B is required for pre-implantation embryonic development by regulating zygotic genome activation. *Cell Prolif* 2024;57(9):e13647.
- [27] Huang da W, Sherman BT, Lempicki RA. Systematic and integrative analysis of large gene lists using DAVID bioinformatics resources. *Nat Protoc* 2009;4(1):44–57.
- [28] Sherman BT, et al. DAVID: a web server for functional enrichment analysis and functional annotation of gene lists (2021 update). *Nucleic Acids Res* 2022;50(W1):W216–21.
- [29] Zhou Y, et al. Metascape provides a biologist-oriented resource for the analysis of systems-level datasets. *Nat Commun* 2019;10(1):1523.
- [30] Wang X, et al. Novel mutations in genes encoding subcortical maternal complex proteins may cause human embryonic developmental arrest. *Reprod Biomed Online* 2018;36(6):698–704.
- [31] Xiong Z, et al. Ultrasensitive Ribo-seq reveals translational landscapes during mammalian oocyte-to-embryo transition and pre-implantation development. *Nat Cell Biol* 2022;24(6):968–80.
- [32] Deng Q, et al. Single-cell RNA-seq reveals dynamic, random monoallelic gene expression in mammalian cells. *Science* 2014;343(6167):193–6.
- [33] Heanue TA, et al. Synergistic regulation of vertebrate muscle development by Dach2, Eya2, and Six1, homologs of genes required for Drosophila eye formation. *Genes Dev* 1999;13(24):3231–43.
- [34] Esteves de Lima J, Relaix F. Master regulators of skeletal muscle lineage development and pluripotent stem cells differentiation. *Cell Regen* 2021;10(1):31.
- [35] Fortin J, et al. Mutant ACVR1 arrests glial cell differentiation to drive tumorigenesis in pediatric gliomas. *Cancer Cell* 2020;37(3):308–23. e12.
- [36] Deng Z, et al. Cdon is essential for organ left-right patterning by regulating dorsal forerunner cells clustering and Kupffer's vesicle morphogenesis. *Front Cell Dev Biol* 2024;12:1429782.
- [37] Li SH, et al. Correlation of cumulus gene expression of GJA1, PRSS35, PTX3, and SERPINE2 with oocyte maturation, fertilization, and embryo development. *Reprod Biol Endocrinol* 2015;13:93.
- [38] Cajas YN, et al. Antioxidant nobilitin enhances oocyte maturation and subsequent embryo development and quality. *Int J Mol Sci* 2020;21(15).
- [39] Stilley JA, et al. Neutralizing TIMP1 restores fecundity in a rat model of endometriosis and treating control rats with TIMP1 causes anomalies in ovarian function and embryo development. *Biol Reprod* 2010;83(2):185–94.
- [40] Chen R, et al. Analyzing embryo dormancy at single-cell resolution reveals dynamic transcriptional responses and activation of integrin-Yap/Taz prosurvival signaling. *Cell Stem Cell* 2024;31(9):1262–79. e8.
- [41] Ozguldeez HO, et al. Polarity inversion reorganizes the stem cell compartment of the trophoblast lineage. *Cell Rep* 2023;42(4):112313.
- [42] Kim EJY, Sorokin L, Hiiragi T. ECM-integrin signalling instructs cellular position sensing to pattern the early mouse embryo. *Development* 2022;149(1).
- [43] Su YQ, et al. Selective degradation of transcripts during meiotic maturation of mouse oocytes. *Dev Biol* 2007;302(1):104–17.
- [44] Zheng P, Dean J. Role of Filia, a maternal effect gene, in maintaining euploidy during cleavage-stage mouse embryogenesis. *Proc Natl Acad Sci U S A* 2009;106(18):7473–8.
- [45] Li J, et al. Genome integrity and neurogenesis of postnatal hippocampal neural stem/progenitor cells require a unique regulator Filia. *Sci Adv* 2020;6(44).